KEY ISSUES REVIEW

Non-Fermi liquids in oxide heterostructures

IOP Publishing Reports on Progress in Physics
Rep. Prog. Phys. **81** (2018) 062502 (12pp) https://doi.org/10.1088/1361-6633/aabdfa

Key Issues Review

Non-Fermi liquids in oxide heterostructures

Susanne Stemmer[1] **and S James Allen**[2]

[1] Materials Department, University of California, Santa Barbara, CA 93106-5050, United States of America
[2] Department of Physics, University of California, Santa Barbara, CA 93106-9530, United States of America

E-mail: stemmer@mrl.ucsb.edu

Received 18 July 2017, revised 25 January 2018
Accepted for publication 13 April 2018
Published 8 May 2018

Corresponding Editor Professor Piers Coleman

Abstract

Understanding the anomalous transport properties of strongly correlated materials is one of the most formidable challenges in condensed matter physics. For example, one encounters metal-insulator transitions, deviations from Landau Fermi liquid behavior, longitudinal and Hall scattering rate separation, a pseudogap phase, and bad metal behavior. These properties have been studied extensively in bulk materials, such as the unconventional superconductors and heavy fermion systems. Oxide heterostructures have recently emerged as new platforms to probe, control, and understand strong correlation phenomena. This article focuses on unconventional transport phenomena in oxide thin film systems. We use specific systems as examples, namely charge carriers in $SrTiO_3$ layers and interfaces with $SrTiO_3$, and strained rare earth nickelate thin films. While doped $SrTiO_3$ layers appear to be a well behaved, though complex, electron gas or Fermi liquid, the rare earth nickelates are a highly correlated electron system that may be classified as a non-Fermi liquid. We discuss insights into the underlying physics that can be gained from studying the emergence of non-Fermi liquid behavior as a function of the heterostructure parameters. We also discuss the role of lattice symmetry and disorder in phenomena such as metal-insulator transitions in strongly correlated heterostructures.

Keywords: strongly correlated materials, oxide heterostructures, non-Fermi liquids, quantum critical points

(Some figures may appear in colour only in the online journal)

1. Introduction

The degree to which the Coulomb interactions among the conduction electrons ('strong correlations') drive novel states of matter in real materials and determine their physical properties lies at the center of many unresolved questions in condensed matter physics. Over the past few years, high-quality thin films and heterostructures have emerged as novel platforms to study strong correlation physics. Heterostructures allow for control of parameters that affect the microscopic physics in ways not possible with bulk materials. For example, carrier densities can be introduced without the use of chemical dopants by modulation doping [1, 2] or polar/non-polar interfaces [3, 4] and tuned through field effect [5–7]. Dimensionality can be controlled through electrostatic confinement coupled with layer-by-layer control. Interfaces can be used to induce magnetism [8] or superconductivity [9], to control lattice symmetry [10], orbital, and charge order [11], phonon coupling, or to create artificial materials in superlattice geometries [12]. Coherency strains in epitaxial structures modify lattice parameters and crystal symmetry, with profound influence on phenomena such as metal-insulator transitions. Advanced thin

film growth approaches yield very high quality films [13]. All of these approaches are now being widely applied to complex oxide materials, including those that are strongly correlated, and have led to many interesting new discoveries.

This article focuses on one specific aspect of correlated oxide heterostructures, namely the electric transport properties of itinerant charge carriers. Deviations from conventional metallic behavior are often referred to as 'non-Fermi liquid', 'strange', or 'bad metal' behavior. These terms describe somewhat different phenomena, and we define them in the following sections, but often they appear within the same materials system. They have been studied for many decades in strongly correlated materials, such as the unconventional superconductors and heavy fermion systems [14–19], using measurements of properties, such as the electrical resistance, thermal transport, or conductivity at optical frequencies, as a function of temperature (T), pressure, doping, frequency, or magnetic field. Often, studies were motivated by the idea that the normal (non-superconducting) state may provide insights into the pairing mechanism that leads to high-temperature superconductivity. Because they remain so profoundly enigmatic, however, in particular when contrasted with the degree of understanding that has been achieved for 'conventional' metals and semiconductors, the transport properties of correlated materials are of high scientific interest in their own right.

The level of difficulty is substantial. For example, in strongly correlated materials, non-Fermi liquid behavior is typically considered in the limit of extremely high carrier concentrations, near one electron/unit cell, where carriers are subject to on-site Coulomb interactions and the material is near a 'Mott' metal insulator transition. These materials are often in proximity to complex magnetically or electronically ordered states. At the other end of the spectrum lie low-density, 2D electron systems in semiconductors, which show unconventional transport and metal-insulator transitions under the influence of long-range Coulomb interactions [20], with the limiting state being the Wigner crystal. How these two extremes intermesh is a subject of ongoing investigation. Strong coupling to the lattice, polaron formation [21], and magnetic interactions are key ingredients of transport in narrow band materials. Disorder, which is always present, can also contribute to non-Fermi liquid behavior [22, 23]. Despite these challenges, several unifying theoretical concepts exist. For example, an underlying quantum critical point can give rise to non-Fermi liquid behavior [14, 15]. The degree to which these concepts apply to a given real material remains, however, a subject of intense debate in many cases.

Only recently have there been substantial efforts to explore correlation phenomena in thin films and heterostructures and in a wider class of materials, beyond high-temperature superconductors [24]. This is in contrast to the study of Coulomb interactions in the very dilute systems, where low-dimensional semiconductors have been the primary focus [25, 26]. The objectives of this article are to use a few specific examples (see figure 1) to discuss the interesting transport phenomena that can be probed in oxide heterostructures and to discuss the insights and new questions that have emerged from these studies. We discuss results from transport studies of quantum wells of $SrTiO_3$, which contain sheet carrier densities on order of 7×10^{14} cm^{-2} confined in a few atomic layers and which exhibit correlated phenomena such as itinerant magnetism, pseudogaps, and metal-insulator transitions [27–30]. We also discuss thin film rare earth nickelates, which exhibit a metal-to-insulator transition upon lowering the temperature [31]. We include in the discussion results from transport studies of doped $SrTiO_3$ for comparison purposes.

2. Scattering rates that show a T^2 temperature dependence

2.1. Longitudinal resistance

The temperature dependence of the electrical resistance of correlated materials typically can be described by power laws. Often a distinction is made between regimes (as a function of some tuning parameter), where the resistance is proportional to T^2, which is the behavior expected for a Fermi liquid at low temperatures, and regimes, where it is proportional to T^n, where n is a 'non-Fermi liquid' exponent with $1 \leqslant n < 2$. While the T^2 Fermi-liquid regime is difficult to detect for conventional metals because it is either overwhelmed by electron-phonon scattering (at high temperatures) or by impurity scattering (at low temperatures) [32], examples of strongly correlated materials that exhibit a pronounced T^2 behavior of the resistance, often to high temperatures, abound. To name a few, they include materials as diverse as V_2O_3 [33], $La_{2-x}Sr_xCuO_4$ [34], $Ag_5Pb_2O_6$ [35], $NdNiO_3$ [36], $NiS_{2-x}Se_x$ [37], and doped $SrTiO_3$ [38]. In some cases, the quadratic temperature dependence reaches room temperature.

A T^2 scattering rate is often taken to be a signature of a 'Fermi liquid'. In a Fermi liquid, electron–electron scattering can give rise to a T^2 behavior, because the phase space for scattering is limited to an energy range of kT around the Fermi energy, E_F, which is a direct consequence of the Pauli exclusion principle. Specifically, for a Fermi liquid [15]:

$$\frac{1}{\tau_{ee}} \sim \frac{\pi}{\hbar}|V|^2 g_F^2 E^2, \tag{1}$$

where τ_{ee} is the quasiparticle lifetime, $\hbar$ is the reduced Planck's constant, $|V|$ is a model-dependent interaction potential, g_F^2 is the density of states at the Fermi surface, and E the energy of the quasiparticle. At finite temperatures, E is set by the temperature, so for quasiparticles near the Fermi surface the scattering rate $(1/\tau_{ee})$ is proportional to T^2. A momentum relaxation mechanism, such as Umklapp scattering, or a complex Fermi surface, are required for electron–electron scattering to influence the resistivity [39, 40]. Here, we discuss recent studies on thin films that show that taking the T^2 behavior to be a signature of a Fermi liquid may not always be correct.

The specific example we discuss here are electron-doped $SrTiO_3$ films. At high temperatures, the mobility of lightly doped $SrTiO_3$ can be described quantitatively by longitudinal optical (LO) phonon scattering of polarons [41–43]. At intermediate temperatures, the resistivity and the Hall mobility show a quadratic temperature dependence (figure 2) [38, 43–45]. The LO phonon scattering is increasingly screened

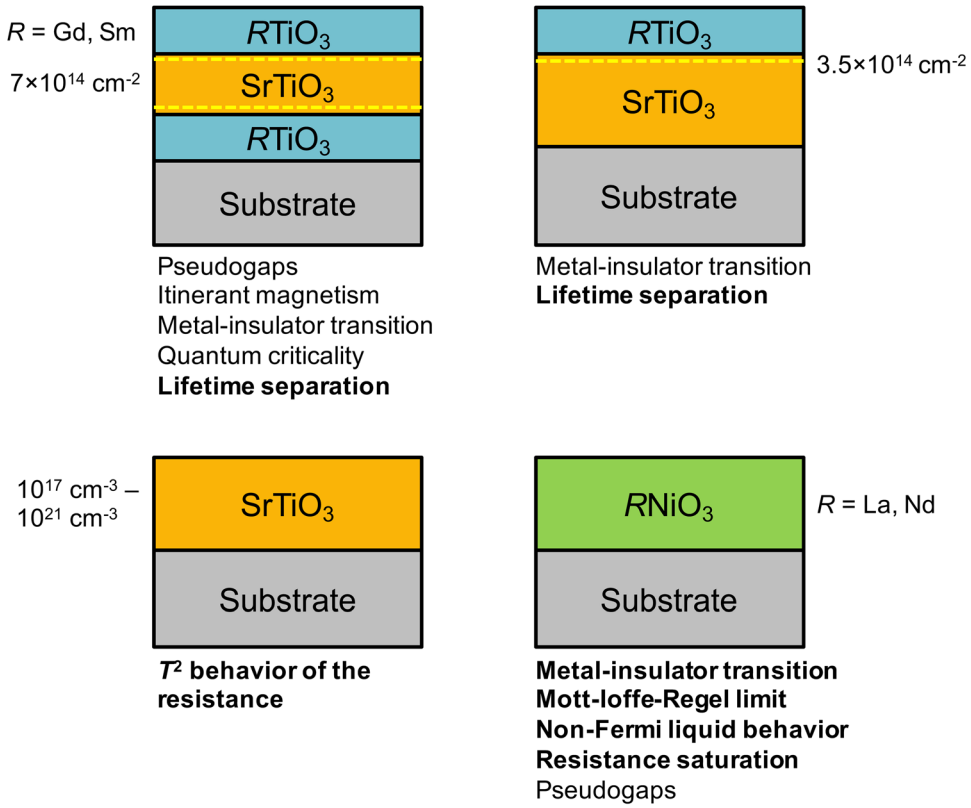

Figure 1. Oxide thin films and heterostructures discussed in this review and some of the phenomena that have been observed (see references in the text). Those that are discussed in more detail here are in bold. The dashed lines indicate the quasi-two-dimensional electron system at the interface between $R\mathrm{TiO_3}$ (R is a rare earth ion but not Eu) and $\mathrm{SrTiO_3}$, which forms as a result of a 'polar discontinuity'. Typical carrier densities are indicated. The thickness of the $\mathrm{SrTiO_3}$ in the quantum well structure can be as low as a single SrO plane sandwiched between the interfacial $\mathrm{TiO_2}$ planes.

as the doping concentration is increased and the T^2 behavior can be observed to higher and higher temperatures [43].

The crux of the matter is that $\mathrm{SrTiO_3}$ shows a T^2 scattering rate at temperatures and electron concentrations where the electron gas is likely non-degenerate [46–49], that is $E_\mathrm{F}(T=0\,\mathrm{K}) \ll k_\mathrm{B}T$, where k_B is the Boltzmann constant or the spacing between the carriers, $N^{-1/3}$, is much greater than the thermal de Broglie wavelength, $h/\sqrt{2\pi m^* k_\mathrm{B} T}$. Here, N is the 3D carrier density, h is Planck's constant, and m^* is the effective carrier mass. $\mathrm{SrTiO_3}$ shows metallic behavior ($\mathrm{d}R/\mathrm{d}T > 0$) even in the non-degenerate case because the dielectric constant (κ), and thus the Bohr radius (a_B), is large, so that the Mott criterion, $Na_\mathrm{B}^3 \sim 0.2$, is fulfilled, where $a_\mathrm{B} = \hbar\kappa/m^*e^2$ (e is the electron charge). If the Fermi level is low, however, the phase space arguments that lead to a T^2 scattering rate in a Fermi liquid according to equation (1) are not applicable. Indeed, in the non-degenerate case the transport is captured by Maxwell-Boltzmann statistics, there is no well-defined Fermi energy and the chemical potential is below the conduction band edge.

If $\mathrm{SrTiO_3}$ shows a T^2 scattering rate even though it is not a Fermi liquid (it is a classical gas) how about other materials? To discuss this question, consider equation (1), which suggests a strong carrier density dependence of $1/\tau_{ee}$, i.e. via the interaction potential. A simpler, phenomenological equation is often used for the scattering rate of a Fermi liquid [50]:

$$\frac{1}{\tau_{ee}} = B \cdot \frac{(k_\mathrm{B}T)^2}{\hbar E_\mathrm{F}}, \tag{2}$$

where B is a dimensionless factor that incorporates scattering event probabilities. $1/\tau_{ee}$ is expected to depend on the carrier density due to E_F (and B). Assuming the resistivity is described by $\rho_{xx} = \rho_0 + AT^2$, where ρ_0 is the residual resistivity, then, according to the Drude model:

$$AT^2 = \frac{m^*}{Ne^2} \cdot \frac{1}{\tau_{ee}}. \tag{3}$$

Measurements of A as a function of carrier density have been reported for several oxides, including cuprates [51–54], vanadates [55], bulk, doped $\mathrm{SrTiO_3}$ [56], and $\mathrm{SrTiO_3}$ quantum wells [56, 57]. In all cases, $A \sim 1/N$, consistent with expectations from the Drude model, see equation (3). A plot that shows this behavior for doped $\mathrm{SrTiO_3}$ appears in figure 3, where $A \sim 1/N$ can be observed over a very large carrier density range in both the non-degenerate and degenerate doping regimes. The important point is that $A \sim 1/N$ means that *the scattering rate*, $1/\tau_{ee}$, is *independent* of the carrier density, contrary to what is expected from Fermi liquid theory, see either equation (1) or equation (2) [56]. Because $A \sim 1/N$ is also observed in materials such as the cuprates which, unlike lightly doped $\mathrm{SrTiO_3}$, can be considered strongly correlated materials, this hints strongly at a surprisingly *universal* T^2 scattering rate that is *not* due to electron–electron scattering in a Fermi liquid.

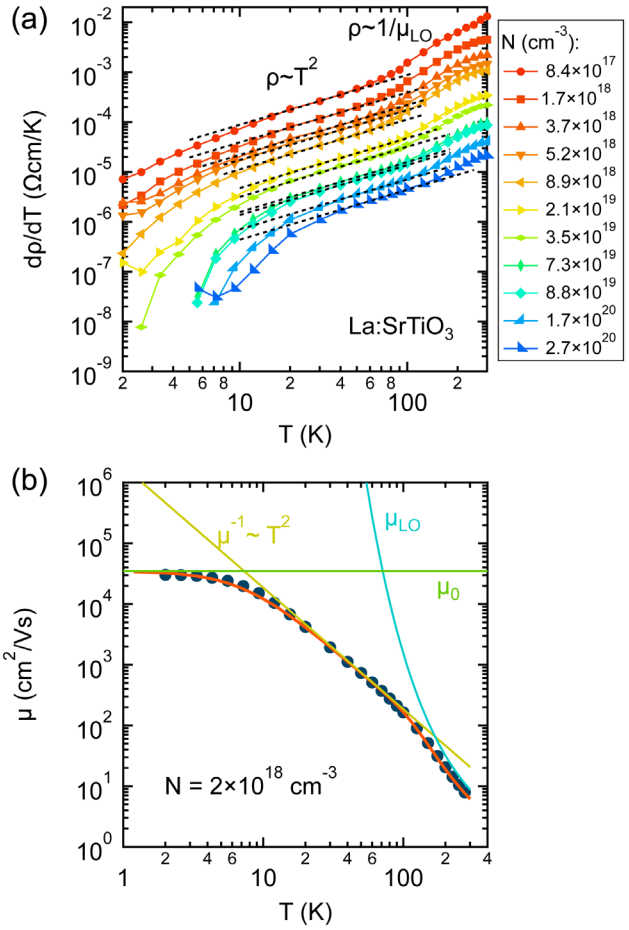

Figure 2. Temperature dependence of the resistivity and Hall mobility of La-doped $SrTiO_3$ films (data from [126]). (a) Log–log plot of the temperature derivative of the resistivity, $\partial\rho/\partial T$, versus temperature, for films with different carrier concentrations. A power law behavior gives a straight line in such a plot. In an intermediate temperature range, the resistivity behaves as T^2, as indicated by the black dashed lines. (b) Hall mobility as a function of temperature for the film with a carrier density of 2×10^{18} cm^{-3} (symbols). As discussed in [43], the mobility can be described completely by just three terms: a temperature-independent impurity scattering term, μ_0, which dominates at low temperatures, a LO phonon-polaron scattering term, μ_{LO}, which dominates at high temperatures, and a term that is proportional to T^{-2}. More details about the LO phonon term can be found in [41]. The results for the fit parameters can be found in [43]. The different lines indicate the contribution of each term and their sum describes the experimental data extremely well, see solid red line. For similar fits for films with different carrier densities, see the supplementary information to [43].

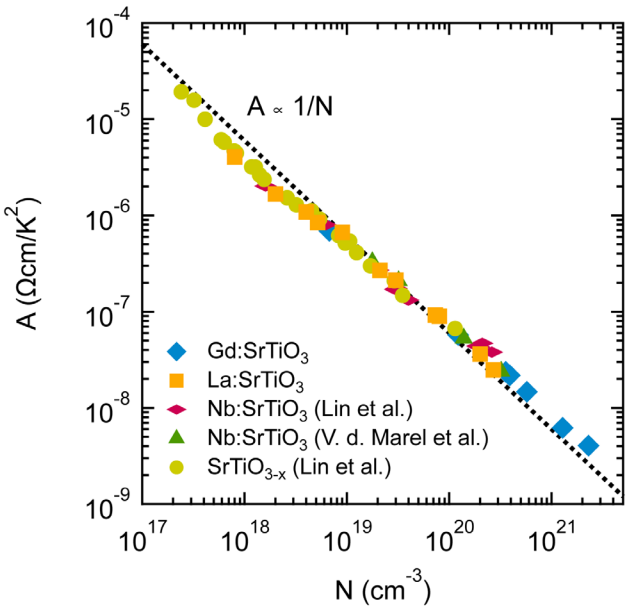

Figure 3. Carrier density dependence of the A-coefficient of the T^2 resistivity term for 3D electron gases in $SrTiO_3$ doped with different dopants (see legend). Data is from thin films (La:$SrTiO_3$ and Gd:$SrTiO_3$) grown by MBE and bulk single crystal data from [44, 45]. The A-coefficient approximately follows a $1/N$ dependence on the carrier density N over orders of magnitude in N, as can be seen by comparison with the black dotted line. Slight deviations from the $1/N$ behavior are expected even if the scattering rate is independent of the carrier density, because the carrier mass also changes as higher lying bands are filled. Reprinted from [56]. CC BY 4.0.

2.2. Hall mobility or Hall angle

Strongly correlated materials often show resistances that depart from the quadratic dependence on temperature (we will discuss these in the next section). In contrast, the Hall angle ($\cot\theta$), which is the inverse of the Hall mobility, almost always shows a very robust T^2 temperature dependence [34, 53, 58–61]. This observation has become known as 'two lifetime' behavior, because it suggests that different scattering rates control the Hall mobility and the longitudinal resistance, respectively [62]. In addition to the cuprates, lifetime separation has been observed in a wide range of correlated materials, including V_2O_3 [63], ruthenates [64, 65], heavy Fermion systems [66, 67], MgB_2 [68], and in oxide heterostructures [57]. Figure 4 shows an example of the two lifetime phenomenon for a high-carrier-density, quasi-two-dimensional electron system at a $SmTiO_3/SrTiO_3$ interface that is close to a metal-insulator transition. Unlike the lightly doped $SrTiO_3$ films discussed in the previous section, this electron system is degenerate. The resistance is ~ $T^{5/3}$ above ~100 K, while the Hall angle is always ~ T^2 [69].

Lifetime separation was also investigated in quantum wells of $SrTiO_3$ [57, 70], such as formed in $SmTiO_3/SrTiO_3/SmTiO_3$ heterostructures, which contain mobile charge densities on order of 7×10^{14} cm^{-2} and which exhibit numerous correlated phenomena, such as itinerant magnetism and pseudogaps, when their thicknesses are reduced to a few atomic planes. These studies showed that the lifetime separation can have two components, namely the different temperature dependencies of Hall angle and longitudinal resistances, as seen in figure 4, but also a divergence in their 0-K residuals [57]. Both lead to a temperature dependence of the Hall coefficient even when there is no major change in the Fermi surface or carrier density. These two contributions to the lifetime separation may have different origins. In the $SrTiO_3$ quantum wells, the divergence of the 0-K scattering rates appeared only near a quantum critical point near a transition to an itinerant magnetic phase [57]. Further analysis of the 0-K residuals suggested that the proximity to the quantum critical point influenced the residual in the Hall angle, but not that of the

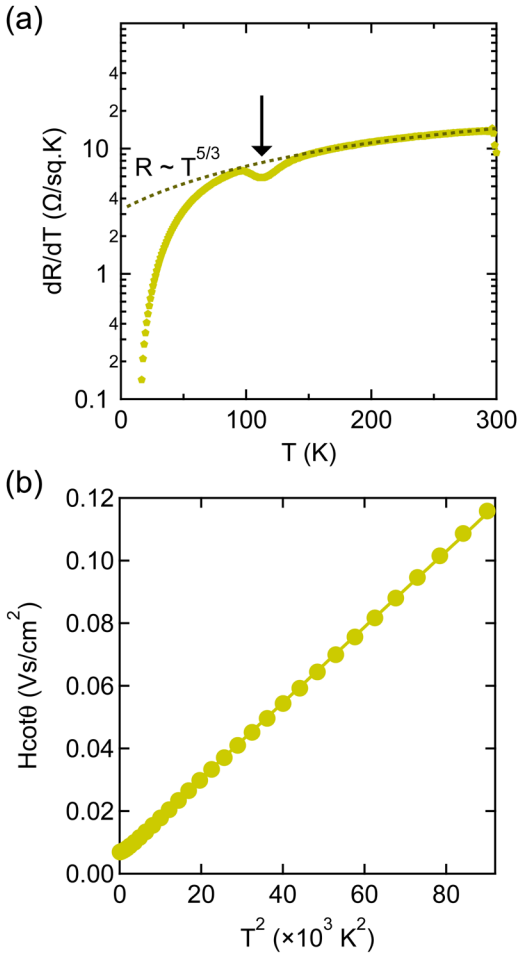

Figure 4. Temperature dependence of the sheet resistance (a) and Hall angle (b) of a quasi-two-dimensional electron liquid at the $SmTiO_3/SrTiO_3$ interface, which has a sheet carrier density of ~2×10^{14} cm^{-2}, due to the polar discontinuity at the interface. The Hall angle, $\cot\theta$, is the inverse of the Hall mobility, μ_H, $H\cot\theta = \mu_H^{-1}$, where H is the magnetic field. The sheet resistance follows a $T^{5/3}$ temperature dependence at elevated temperatures, then shows a dip, followed by a small temperature interval of ~T^2 temperature dependence, and an upturn at low temperatures. In contrast to the complicated behavior of the resistance, the Hall angle follows a T^2 temperature dependence almost over the entire temperature range. Note that the LO phonon scattering term at high temperatures, which is clearly seen for the low density, 3D electron gas in figure 1(b), is absent here, due to the screening of the LO phonons at the high electron density. Data is from [69].

longitudinal resistance. In the cuprates, the 0-K divergence in scattering rates has been explained with anisotropies in the elastic scattering rates [71]. In a recent study of $SmTiO_3/SrTiO_3/SmTiO_3$ quantum wells, we showed that disorder affected the residuals in both the Hall angle and longitudinal resistances, but it did not affect their 0-K divergence [70].

There currently exists no generally accepted understanding of lifetime separation [72]. Suggested explanations include a 2D Luttinger liquid (spin-charge separation), complex Fermi surfaces combined with strongly anisotropic scattering rates, as may occur near an antiferromagnetic transition, bipolarons, and quantum critical points [18, 54, 62, 73–78]. Most theoretical models aimed at reproducing $R \sim T$ and $\cot\theta \sim T^2$, which, unfortunately, does not apply to all of the materials for which lifetime separation is observed, such as the $SrTiO_3$ interfacial electron systems. One point of view is to take the T^2 Hall scattering rate as a signature of an underlying Fermi liquid state even though the resistance departs from simple behavior [53]. In the light of what was discussed above, namely that a T^2 scattering rate *may not* always indicate a Fermi liquid, this interpretation should be taken with some degree of caution.

To summarize section 2, there are a surprising number of common features in the transport of a wide range of correlated materials and complex oxide heterostructures: a Hall angle (inverse of the Hall mobility) that remains robustly T^2, independent of the specific temperature dependence of the longitudinal resistance, and a scattering rate that does not appear to be overly sensitive to factors such as the carrier density, electronic structure, or even whether the electron system is degenerate or non-degenerate. Coupling to the lattice should certainly be considered in any future developments of an understanding of the unusual transport properties of oxides, as will also be discussed in the following sections. The quasiparticle mass in $SrTiO_3$ at low temperatures is enhanced by a factor of two, most likely due to dressing by phonons [79], as is also seen in angle resolved photoemission [80]. Similar to electron–electron scattering in metals [32], the pronounced T^2 scattering rate, which often extends to very high temperatures, appears to be a feature for electrons in conduction bands derived from *d*-states. For example, a degenerate perovskite oxide system with an s-band conduction band, La-doped $BaSnO_3$, does not exhibit a T^2 scattering rate in its resistance [81]. The findings illustrate the need for a theoretical framework that can explain (*i*) the universal T^2 scattering rate and, equally important, (ii) its peculiar robustness in the Hall angle. By universal we mean that it encompasses high-carrier-density, correlated materials as well as low-density systems such as $SrTiO_3$.

3. T^n power laws in the electrical resistivity

Departures from T^2 behavior in the longitudinal resistance to other power laws of form T^n, with $1 \leqslant n \leqslant 2$ are ubiquitous. These power laws are often identified as signatures of 'non-Fermi liquids'. The extreme case are the superconducting cuprates, which show *T*-linear behavior in the normal state, sometime referred to as 'strange metal' behavior.

One possible explanation for non-Fermi liquid behavior are quantum critical points [15]. Near a magnetic or other instability, the associated order parameter fluctuations may lead to strong scattering and non-Fermi-liquid behavior [82]. Oxide heterostructures allow for testing these ideas by using tuning parameters, such as epitaxial strain, to bring a material system close to a quantum critical point. Here, we discuss results from epitaxial $NdNiO_3$ films.

Metallic rare earth nickelates (except $LaNiO_3$) possess an orthorhombic perovskite-derived crystal structure (space group P*bnm*). They exhibit temperature-driven metal-insulator transitions, whose transition temperature depends on the size of the rare earth ion and degree of oxygen octahedral tilts in the orthorhombic structure, which control the bandwidth [31].

The symmetry of the insulating, low-temperature, antiferromagnetic phase is monoclinic ($P2_1n$) [83, 84]. In this space group, the presence of two inequivalent Ni sites allow for 1:1 charge order [85] (or 'bond-length disproportionation', since the actual charge on the two Ni sites may not be very different [86, 87]). The electrical resistivity of the rare earth nickelates above the metal-insulator transition exhibits T^n behavior and various exponents of $n \sim 4/3$, 5/3, or 2 have been reported [36, 88–90]. The rare earth nickelates are therefore an interesting system to investigate various power laws in transport in proximity to metal-insulator transitions.

As shown in [36], the temperature dependence of the resistivity of the rare earth nickelates in the metallic phase can be described by the following equation:

$$\frac{1}{\rho} = \frac{1}{\rho_{\text{ideal}}} + \frac{1}{\rho_{\text{sat}}}, \tag{4}$$

where ρ_{sat} is a saturation resistivity. As will be discussed in the next section, resistivity saturation is important in modeling transport when the scattering rate is high and ρ_{ideal} becomes large. Although there are materials that do not show saturation, neglecting ρ_{sat} [89, 91] in case of the nickelates yields incorrect values for n [36]. In many correlated materials, ρ_{ideal} is described by a power law:

$$\rho_{\text{ideal}} = \rho_0 + AT^n. \tag{5}$$

Figure 5 shows results for epitaxial $NdNiO_3$ films, which were coherently strained to substrates having different signs and degrees of lattice mismatch [36]. It was shown that n assumes just two values, either $n = 2$ or $n = 5/3$ [36]. Specifically, if the metal-insulator transition was suppressed, which is the case for in-plane compressive strains, then $n = 5/3$. Electron diffraction studies showed that films under compressive strains adopt space group $P2_1m$ [92], which is expected from symmetry arguments discussed in [93]. The $P2_1m$ space group does not allow for 1:1 charge order, which would require further lowering of the symmetry [92], which is not possible in films that are coherently constrained to a substrate. In contrast, films under tensile strain possess orthorhombic symmetry, which allows for the transition to the charge ordered, insulating state [92].

Thus, thin film studies establish the following about this strongly correlated system: (i) the metal-insulator transition in the rare earth nickelates is suppressed if the heterostructure boundary conditions prevent establishment of 1:1 charge order. In other words, 1:1 charge order is a requirement for the insulating state. (ii) The non-Fermi liquid exponent of $n = 5/3$ is associated with the suppression of the 1:1 charge ordered insulating state. On first sight, (ii) appears consistent with theories that ascribe non-Fermi liquid exponents to order parameter fluctuations; in this case it may be associated with the suppression of charge and antiferromagnetic order, and a nearby quantum critical point. Interestingly, both types of metals (both symmetries) exhibit pseudogaps (a depletion of the single particle density of states), which, in the case when the insulator is not suppressed, develops into a full gap [94]. Pseudogaps are typically associated with incipient antiferromagnetic order. We note, however, that there are just two

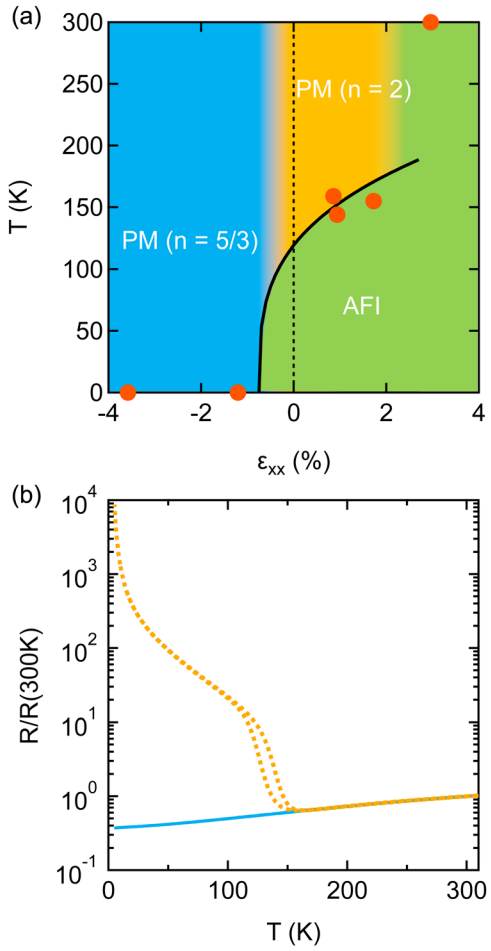

Figure 5. (a) Phase diagram for strained $NdNiO_3$ thin films (film thickness: ~15 pseudocubic unit cells). The horizontal axis indicates the in-plane epitaxial film strain. The data points indicate the metal-insulator transition temperatures. The film with the data point at 300 K was insulating at all measured temperatures. The different colors indicate the regimes where the metallic phase shows different power law exponents n in the temperature dependences of the resistance, which are indicated. PM = paramagnetic metal and AFI = antiferromagnetic insulator. (b) Examples of the basic behaviors, showing a film that undergoes a temperature-driven metal-insulator transition and one where the transition is completely suppressed by the compressive epitaxial in-plane strain. Reproduced from [36]. CC BY 4.0.

exponents observed in the entire phase diagram in figure 4. This observation points to a picture of specific, fractional exponents in the temperature dependence of the resistivity that are firmly tied to a specific non-Fermi liquid phase, with a distinct symmetry. A similar case of a 'non-Fermi liquid phase' has been made previously for the itinerant ferromagnet MnSi [95].

4. Mott–Ioffe–Regel-limit and resistance saturation

At high temperatures, two types of behaviors of the electrical resistance of high-resistance materials can be distinguished: (i) the resistance increases seemingly without limit or (ii) it 'saturates' by slowly approaching a finite value. The

non-saturating behavior (i) has become known as 'bad metal behavior' [96]. It has attracted attention because unconventional superconductors in their normal state are non-saturating and it is considered a signature of a novel kind of metallic state [96]. Neither case is, however, fully understood [97–104]. Confusion arises from the fact that the Mott–Ioffe–Regel limit appears in the discussion, so we discuss this briefly first.

4.1. Mott–Ioffe–Regel limit

The resistances of thin metal oxide films are often sufficiently high that they reach or exceed the Mott–Ioffel–Regel limit. This limit is the resistance when the scattering of the carriers becomes so strong that $lk_F \sim 1$, where l is the mean free path of the carriers and k_F the Fermi wave vector [105, 106]. An approximate value for the Mott–Ioffe–Regel limit in two dimensions is h/e^2 [107]. It is well-established to be relevant in the regime of elastic scattering *at low temperatures*, i.e. it establishes a criterion where a plane wave description no longer makes any sense [26, 104]. A 2D electron system that, for any reason, exceeds a sheet resistance on order of of h/e^2 (25 kΩ/sq.) at low temperatures may thus be expected to be localized. In three dimensions, there is an additional factor k_F^{-1} [107]. In keeping with this expected behavior, there are ubiquitous observations of oxide thin films and heterostructures that exhibit insulating behavior at all temperatures at low film thicknesses, because their resistance exceeds the Mott–Ioffe–Regel limit [108–111]. Figure 6 shows an example of this behavior for a $LaNiO_3$ film [112]. The point here is that the observation of insulating behavior in such cases should not be used as evidence of a correlation-induced metal-insulator transition. Often, the resistivity also increases as the film thickness is reduced. This can be due to a number of reasons, such as increased scattering from surfaces and interfaces. Another reason is bandwidth narrowing, which is related to the octahedral tilts in the distorted perovskite structure that these oxides adopt. Connectivity with the substrate and film strain all affect the octahedral tilts [10, 113]. For example, thin $LaNiO_3$ films exhibit octahedral tilt patterns near the interface with a substrate that are different from those in the bulk and which cause a high resistivity, and insulating behavior below a critical thickness as the Mott–Ioffe–Regel limit is exceeded. In contrast, $LaNiO_3$ films of the same thickness embedded in superlattices remain metallic, which can be explained with their different octahedral tilt patterns [113]. Films further in the metallic regime typically show weak localization behavior [114] at low temperatures, which is manifested as an upturn in the resistance at low temperatures, also seen in figure 6.

One unfortunate consequence of the high resistances in thin films due to the inherently low carrier mobilities of correlated materials, and associated localization when the Mott–Ioffe–Regel limit is exceeded, is that it makes it difficult to study correlation effects in *itinerant*, low-dimensional systems, which are pre-empted by this 'trivial' localization. An example of interesting phenomena that may emerge when resistances are kept well below the Mott–Ioffe–Regel limit is a novel metal-insulator transition in an interfacial electron system at the $SmTiO_3/SrTiO_3$ interface [69].

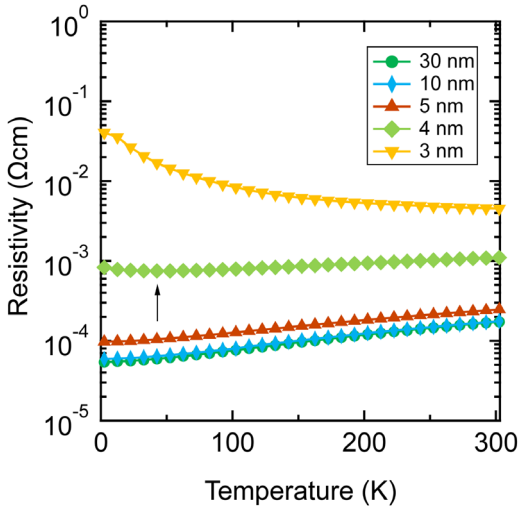

Figure 6. Resistivity as a function of temperature for $LaNiO_3$ films of different thickness. The films were grown on LSAT [$(La_{0.3}Sr_{0.7})(Al_{0.65}Ta_{0.35})O_3$] substrates. In bulk, $LaNiO_3$ is a metal at all temperatures, and does not show a temperature-induced metal insulator transition, unlike the other rare earth nickelates. The thinnest (3 nm) film exceeds the Mott–Ioffe–Regel limit and is insulating at all temperatures. Its sheet resistance is about 15 kΩ at room temperature. The sheet resistance of the next-thinnest film (4 nm thickness) significantly lower, ~2700 Ω. It shows an upturn in the resistivity at low temperatures, which could be due to weak localization (see arrow). The resistances of $LaNiO_3$ films are very sensitive to modification of octahedral tilt patterns by the substrate and adjacent layers. Ultrathin $LaNiO_3$ films in superlattice geometries, which have different tilt patterns than those directly adjacent to a rigid substrate, remain metallic (they do not exceed the Mott–Ioffe–Regel limit) [113]. Reprinted with permission from [112]. Copyright (2010), AIP Publishing LLC.

4.2. High temperatures: saturating and non-saturating metals

Returning to the high temperature characteristics, we remark that at high temperatures the scattering is largely inelastic. Multiple scattering and phase coherence, features of transport at the low temperature localization transition are not important at high temperature. Saturating metals are well described by the parallel resistor formula, equation (4). This formula emerges in a transport model that invokes the Mott–Ioffe–Regel limit as a cut-off time, τ_0, for the mean time between electron scattering, $\tau > \tau_0 = a/v_F$ [115]. The physical basis of this model is that it suggests there should be no transport time scale shorter than the time it takes an electron to move across a unit cell. Following [115], Hussey *et al* use this approach with some modifications to obtain the parallel resistor model as well as an intuitive frequency dependent conductivity that consists of a Drude response that is broadened and disappears at high temperature leaving a broad incoherent tail that extrapolates to ρ_{sat}^{-1} at low frequency [104]. Time scales, high frequency dynamics, and incoherent high frequency tails are discussed in [102]. While ρ_{sat} invokes the Mott–Ioffe–Regel criterion, its precise value for any given system is determined by important details. Since ρ_{sat} is an important feature

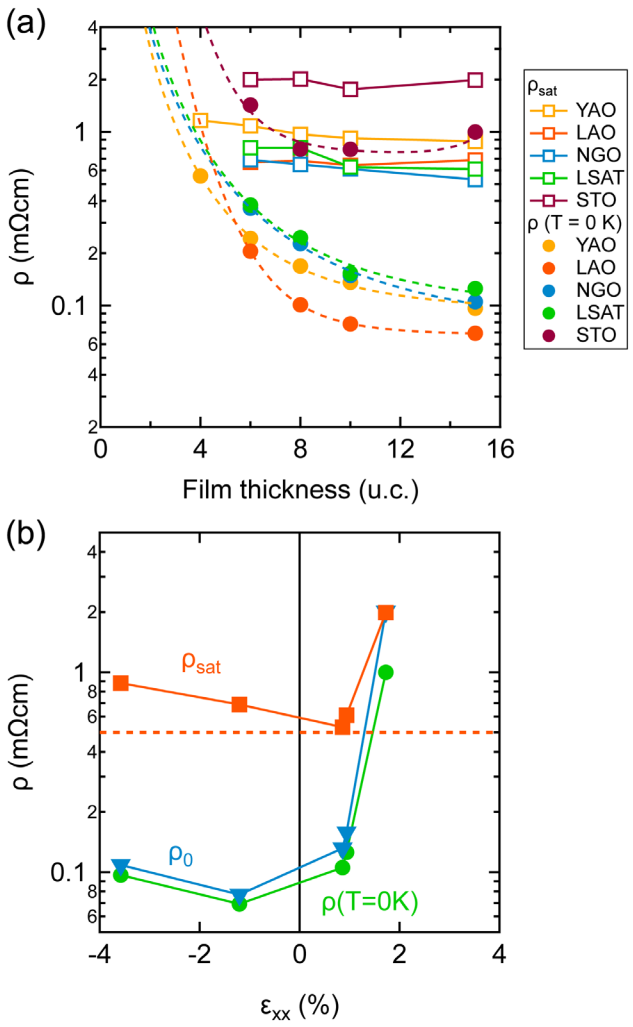

Figure 7. Evolution of the fit parameters in equations (4) and (5) for strained $NdNiO_3$ films with film thickness (a) and in-plane film strain (b). The thickness of the $NdNiO_3$ films in (b) is 15 pseudocubic unit cells (u.c.) and their phase diagram was shown in figure 5. Substrates are $YAlO_3$ (YAO), $LaAlO_3$ (LAO), $NdGaO_3$ (NGO), $(LaAlO_3)_{0.3}(Sr_2AlTaO_6)_{0.7}$ (LSAT), and $SrTiO_3$ (STO), imposing in-plane epitaxial strains of −3.58% (YAO), −1.20% (LAO), +0.86% (NGO), +0.93% (LSAT) and +1.72% (STO), respectively. The dashed horizontal line in (b) is a simple estimate of the Mott–Ioffe–Regel limit. The disorder contribution to the resistivity, $\rho_0 \sim \rho\,(0\,\mathrm{K})$ increases with decreasing film thickness, while the saturation resistance is not strongly affected. Both ρ_0 and ρ_{sat} are strain dependent, establishing a connection between the electronic structure and ρ_{sat}. Reproduced from [36]. CC BY 4.0.

in complex materials, estimates of the expected value of the maximum scattering rate and the other material parameters that determine the saturated conductivity need to be taken with a grain of salt and can differ from reasonable estimates by orders of magnitude.

It is important to appreciate that the effect of scattering rate saturation and ρ_{sat} will emerge in the experimental measurement well below resistivity saturation and must be included in fits to experimental data to extract ρ_{ideal}, as was emphasized in section 3. The degree to which it affects the data depends on the relative values of ρ_{sat}, ρ_0, and A. Figure 7 shows these values for the $NdNiO_3$ films discussed in section 3 [36]. ρ_{sat} increases with increasing epitaxial coherency strain. Strains lift the orbital degeneracy of the Ni e_g states [116, 117], and the magnitude of ρ_{sat} is sensitive to these changes in the electronic structure. Furthermore, while ρ_0 increases sharply with decreasing film thickness, ρ_{sat} is insensitive to it. This results in a critical film thickness for each mismatch strain at which the condition $\rho_{sat} \sim \rho_0$ is fulfilled, and these films are insulating. This can be understood from equation (4): if $\rho_{sat} \sim \rho_0$, then the first term becomes small at finite temperatures compared to $1/\rho_{sat}$, which represents the incoherent (non-Drude) part, and such a film cannot be a metal anymore.

We finally note that while much theoretical effort has been expended to understand the *absence* of resistance saturation in some *degenerate* electron liquids [97–100, 104], so called 'bad metals', the absence of resistance saturation at high temperatures in low-density $SrTiO_3$, is probably neither 'strange' or 'bad', contrary to [118]. The system is a *non-degenerate* electron gas and as such is described by Maxwell-Boltzmann statistics. Assuming a mean free path no shorter than a unit cell dimension, $\sim a$, the shortest effective scattering time, τ, may be related to the thermal velocity, v_{th}, as $\tau = a/v_{th}$. The thermal velocity, $v_{th} = (2k_BT/m^*)^{1/2}$ increases as $T^{1/2}$ and one can estimate the temperature dependent *upper bound* to the high temperature resistivity by $\rho_{sat} \approx \left[m^*(T)/ne^2\right]\left[v_{th}/a\right]$. We expect no saturation of the high temperature resistivity for this non-degenerate system; 'ρ_{sat}' would increase with temperature. Furthermore, transport in $SrTiO_3$ at high temperatures is described by large polarons and one expects a strong increase in effective mass [119–121]. The experimental data shows that the resistivity rises substantially faster than that given by the temperature dependence of v_{th} alone, indicating an increase in m^*. Taking a mass of $\sim 5m^*$ at room temperature, we estimate a room temperature resistivity bound of ~5 Ω cm at an electron concentration of $\sim 4 \times 10^{17}$ cm^{-3}. The data in [118] does not violate this bound. Alternatively, one can take the room temperature resistivity of $\sim 4 \times 10^{17}$ cm^{-3}, and a thermal velocity based on a mass of $\sim 5m^*$ and extract a mean free path of roughly $\sim 2a$. If we accept these assumptions, low-doped $SrTiO_3$ is a well-behaved semiconductor at room temperature and not a bad or strange metal.

We also note that Boltzmann theory applies for phonon scattering in metals at most temperatures [122], even though the room temperature scattering rate is very large, $\sim k_BT/\hbar$ [123–125]. Indeed, the high temperature mobility of doped $SrTiO_3$ can be quantitatively described by a gas of polarons that scatters on LO phonons [42, 43], even though it has a very large scattering rate.

5. Conclusions

In summary, anchoring our discussion with transport in doped $SrTiO_3$, which appears to be a well-behaved electron gas or liquid albeit with a poorly understood T^2 scattering rate, other oxide heterostructures and thin films exhibit many non-Fermi liquid phenomena, such as power laws in the temperature dependence of the resistance, lifetime separation, and resistance saturation. Because of the additional degrees of freedom, thin film studies

allow for illuminating key questions, such as the role of coupling to the lattice in the transport behavior. While some phenomena, such as localization as resistances exceed the Mott–Ioffe–Regel limit, can be understood based in classical models, many others cannot be captured even qualitatively within the framework of existing descriptions of transport. These include the robust and surprisingly universal T^2 dependence of the Hall angle and fractionalized non-Fermi liquid exponents that signify new phases. It is obvious that a new description of charge carrier transport and interactions is likely needed that applies and generalizes to a much wider class of materials than those traditionally considered in the existing models of non-Fermi liquid behavior.

Acknowledgments

The authors acknowledge the US Army Research Office (grant number W911NF-14-1-0379), FAME, one of six centers of STARnet, a Semiconductor Research Corporation program sponsored by MARCO and DARPA, and the US Department of Energy (grant number DEFG02-02ER45994) for support and Evgeny Mikheev for preparing several of the figures. We also thank the many students and postdocs, whose research enabled this article, especially: Evgeny Mikheev, Jack Zhang, Junwoo Son, Jinwoo Hwang, Kaveh Ahadi, Patrick Marshall, Santosh Raghavan, Pouya Moetakef, Clayton Jackson, Adam Kajdos, Tyler Cain, and Adam Hauser.

ORCID iDs

Susanne Stemmer https://orcid.org/0000-0002-3142-4696
S James Allen https://orcid.org/0000-0002-9858-255X

References

[1] Son J, Jalan B, Kajdos A P, Balents L, Allen S J and Stemmer S 2011 Probing the metal–insulator transition of $NdNiO_3$ by electrostatic doping *Appl. Phys. Lett.* **99** 192107
[2] Kajdos A P, Ouellette D G, Cain T A and Stemmer S 2013 Two-dimensional electron gas in a modulation-doped $SrTiO_3$/Sr(Ti,Zr)O_3 heterostructure *Appl. Phys. Lett.* **103** 082120
[3] Ohtomo A and Hwang H Y 2004 A high-mobility electron gas at the $LaAlO_3$/$SrTiO_3$ heterointerface *Nature* **427** 423–6
[4] Stemmer S and Allen S J 2014 Two-dimensional electron gases at complex oxide interfaces *Annu. Rev. Mater. Res.* **44** 151–71
[5] Ahn C H *et al* 2006 Electrostatic modification of novel materials *Rev. Mod. Phys.* **78** 1185–212
[6] Ahn C H, Gariglio S, Paruch P, Tybell T, Antognazza L and Triscone J M 1999 Electrostatic modulation of superconductivity in ultrathin $GdBa_2Cu_3O_{7-x}$ films *Science* **284** 1152–5
[7] Newns D M, Misewich J A, Tsuei C C, Gupta A, Scott B A and Schrott A 1998 Mott transition field effect transistor *Appl. Phys. Lett.* **73** 780–2
[8] Hellman F *et al* 2017 Interface-induced phenomena in magnetism *Rev. Mod. Phys.* **89** 025006
[9] Gozar A, Logvenov G, Kourkoutis L F, Bollinger A T, Giannuzzi L A, Muller D A and Bozovic I 2008 High-temperature interface superconductivity between metallic and insulating copper oxides *Nature* **455** 782–5
[10] Rondinelli J M, May S J and Freeland J W 2012 Control of octahedral connectivity in perovskite oxide heterostructures: an emerging route to multifunctional materials discovery *MRS Bull.* **37** 261–70
[11] Frano A *et al* 2016 Long-range charge-density-wave proximity effect at cuprate/manganate interfaces *Nat. Mater.* **15** 831–4
[12] May S J, Santos T S and Bhattacharya A 2009 Onset of metallic behavior in strained $(LaNiO_3)_n$/$(SrMnO_3)_2$ superlattices *Phys. Rev.* B **79** 115127
[13] Schlom D G 2015 Perspective: Oxide molecular-beam epitaxy rocks! *APL Mater.* **3** 062403
[14] Sachdev S 2014 *Quantum Phase Transitions* 2nd edn (Cambridge: Cambridge University Press)
[15] Schofield A J 1999 Non-Fermi liquids *Contemp. Phys.* **40** 95–115
[16] Varma C M, Nussinov Z and van Saarloos W 2002 Singular or non-Fermi liquids *Phys. Rep.* **361** 267–417
[17] Metzner W, Castellani C and Castro C D 1998 Fermi systems with strong forward scattering *Adv. Phys.* **47** 317–445
[18] Anderson P W 1995 New physics of metals: Fermi surfaces without Fermi liquids *Proc. Natl Acad. Sci.* **92** 6668–74
[19] Stewart G R 2001 Non-Fermi-liquid behavior in d- and f-electron metals *Rev. Mod. Phys.* **73** 797–855
[20] Spivak B, Kravchenko S V, Kivelson S A and Gao X P A 2010 Colloquium: Transport in strongly correlated two dimensional electron fluids *Rev. Mod. Phys.* **82** 1743–66
[21] Emin D 2013 *Polarons* (Cambridge: Cambridge University Press)
[22] Miranda E and Dobrosavljevic V 2005 Disorder-driven non-Fermi liquid behaviour of correlated electrons *Rep. Prog. Phys.* **68** 2337–408
[23] Belitz D and Kirkpatrick T R 1994 The Anderson–Mott transition *Rev. Mod. Phys.* **66** 261–390
[24] Chakhalian J, Freeland J W, Millis A J, Panagopoulos C and Rondinelli J M 2014 Colloquium: emergent properties in plane view: strong correlations at oxide interfaces *Rev. Mod. Phys.* **86** 1189–202
[25] Kravchenko S V and Sarachik M P 2004 Metal–insulator transition in two-dimensional electron systems *Rep. Prog. Phys.* **67** 1–44
[26] Lee P A and Ramakrishnan T V 1985 Disordered electronic systems *Rev. Mod. Phys.* **57** 287–337
[27] Moetakef P, Jackson C A, Hwang J, Balents L, Allen S J and Stemmer S 2012 Toward an artificial Mott insulator: correlations in confined high-density electron liquids in $SrTiO_3$ *Phys. Rev.* B **86** 201102
[28] Jackson C A and Stemmer S 2013 Interface-induced magnetism in perovskite quantum wells *Phys. Rev.* B **88** 180403
[29] Marshall P B, Mikheev E, Raghavan S and Stemmer S 2016 Pseudogaps and emergence of coherence in two-dimensional electron liquids in $SrTiO_3$ *Phys. Rev. Lett.* **117** 046402
[30] Need R F, Isaac B J, Kirby B J, Borchers J A, Stemmer S and Wilson S D 2016 Interface-driven ferromagnetism within the quantum wells of a rare earth titanate superlattice *Phys. Rev. Lett.* **117** 037205
[31] Torrance J B, Lacorre P, Nazzal A I, Ansaldo E J and Niedermayer C 1992 Systematic study of insulator-metal transitions in perovskites $RNiO_3$ (R = Pr,Nd,Sm,Eu) due to closing of charge-transfer gap *Phys. Rev.* B **45** 8209–12
[32] Kaveh M and Wiser N 1984 Electron-electron scattering in conducting materials *Adv. Phys.* **33** 257–372
[33] McWhan D B and Rice T M 1969 Critical pressure for the metal–semiconductor transition in V_2O_3 *Phys. Rev. Lett.* **22** 887–90

[34] Ando Y, Kurita Y, Komiya S, Ono S and Segawa K 2004 Evolution of the Hall coefficient and the Peculiar electronic structure of the cuprate superconductors *Phys. Rev. Lett.* **92** 197001

[35] Yonezawa S and Maeno Y 2004 Nonlinear temperature dependence of resistivity in single crystal $Ag_5Pb_2O_6$ *Phys. Rev.* B **70** 184523

[36] Mikheev E, Hauser A J, Himmetoglu B, Moreno N E, Janotti A, Van de Walle C G and Stemmer S 2015 Tuning bad metal and non-Fermi liquid behavior in a Mott material: rare earth nickelate thin films *Sci. Adv.* **1** e1500797

[37] Honig J M and Spalek J 1998 Electronic properties of $NiS_{2-x}Se_x$ single crystals: from magnetic Mott–Hubbard insulators to normal metals *Chem. Mater.* **10** 2910–29

[38] Baratoff A and Binnig G 1981 Mechanism of superconductivity in $SrTiO_3$ *Physica B + C* **108** 1335–6

[39] Pal H K, Yudson V I and Maslov D L 2012 Resistivity of non-Galilean-invariant Fermi- and non-Fermi liquids *Lith. J. Phys.* **52** 142–64

[40] Gurzhi R N 1965 Some features of the electrical conductivity of metals at low temperatures *Sov. Phys. JETP* **20** 953–60

[41] Frederikse H P R and Hosler W R 1967 Hall mobility in $SrTiO_3$ *Phys. Rev.* **161** 822–7

[42] Verma A, Kajdos A P, Cain T A, Stemmer S and Jena D 2014 Intrinsic mobility limiting mechanisms in lanthanum-doped strontium titanate *Phys. Rev. Lett.* **112** 216601

[43] Mikheev E, Himmetoglu B, Kajdos A P, Moetakef P, Cain T A, Van de Walle C G and Stemmer S 2015 Limitations to the room temperature mobility of two- and three-dimensional electron liquids in $SrTiO_3$ *Appl. Phys. Lett.* **106** 062102

[44] van der Marel D, van Mechelen J L M and Mazin I I 2011 Common Fermi-liquid origin of T^2 resistivity and superconductivity in n-type $SrTiO_3$ *Phys. Rev.* B **84** 205111

[45] Lin X, Fauqué B and Behnia K 2015 Scalable T^2 resistivity in a small single-component Fermi surface *Science* **349** 945–8

[46] Shirai K and Yamanaka K 2013 Mechanism behind the high thermoelectric power factor of $SrTiO_3$ by calculating the transport coefficients *J. Appl. Phys.* **113** 053705

[47] Jalan B and Stemmer S 2010 Large Seebeck coefficients and thermoelectric power factor of La-doped $SrTiO_3$ thin films *Appl. Phys. Lett.* **97** 042106

[48] Swift M W and Van de Walle C G 2017 Conditions for T^2 resistivity from electron–electron scattering *Eur. Phys. J.* B **90** 151

[49] Maslov D L and Chubukov A V 2017 Optical response of correlated electron systems *Rep. Prog. Phys.* **80** 026503

[50] Ashcroft N W and Mermin N D 1976 *Solid State Physics* (Belmont: Brooks/Cole)

[51] Hussey N E, Gordon-Moys H, Kokalj J and McKenzie R H 2013 Generic strange-metal behaviour of overdoped cuprates *J. Phys.: Conf. Ser.* **449** 012004

[52] Barisic N, Chan M K, Li Y, Yu G, Zhao X, Dressel M, Smontara A and Greven M 2013 Universal sheet resistance and revised phase diagram of the cuprate high-temperature superconductors *Proc. Natl Acad. Sci.* **110** 12235–40

[53] Li Y, Tabis W, Yu G, Barišić N and Greven M 2016 Hidden Fermi-liquid charge transport in the antiferromagnetic phase of the electron-doped cuprate superconductors *Phys. Rev. Lett.* **117** 197001

[54] Lee D K K and Lee P A 1997 Transport phenomenology for a holon–spinon fluid *J. Phys.: Condens. Matter* **9** 10421–8

[55] Oka D, Hirose Y, Nakao S, Fukumura T and Hasegawa T 2015 Intrinsic high electrical conductivity of stoichiometric $SrNbO_3$ epitaxial thin films *Phys. Rev.* B **92** 205102

[56] Mikheev E, Raghavan S, Zhang J Y, Marshall P B, Kajdos A P, Balents L and Stemmer S 2016 Carrier density independent scattering rate in $SrTiO_3$-based electron liquids *Sci. Rep.* **6** 20865

[57] Mikheev E, Freeze C R, Isaac B J, Cain T A and Stemmer S 2015 Separation of transport lifetimes in $SrTiO_3$-based two-dimensional electron liquids *Phys. Rev.* B **91** 165125

[58] Chien T R, Wang Z Z and Ong N P 1991 Effect of Zn impurities on the normal-state Hall angle in single-crystal $YBa_2Cu_{3-x}Zn_xO_{7-\partial}$ *Phys. Rev. Lett.* **67** 2088–91

[59] Carrington A, Mackenzie A P, Lin C T and Cooper J R 1992 Temperature-dependence of the Hall angle in single-crystal $YBa_2(Cu_{1-x}Co_x)_3O_{7-\partial}$ *Phys. Rev. Lett.* **69** 2855–8

[60] Ogino M, Watanabe T, Tokiwa H, Iyo A and Ihara H 1996 Hall effect of superconducting copper oxide, Cu-1234 *Physica* C **258** 384–8

[61] Xiao G, Xiong P and Cieplak M Z 1992 Universal Hall effect in $La_{1.85}Sr_{0.15}Cu_{1-x}A_xO_4$ systems (A = Fe,Co,Ni,Zn,Ga) *Phys. Rev.* B **46** 8687

[62] Anderson P W 1991 Hall-effect in the 2-dimensional Luttinger liquid *Phys. Rev. Lett.* **67** 2092–4

[63] Rosenbaum T F, Husmann A, Carter S A and Honig J M 1998 Temperature dependence of the Hall angle in a correlated three-dimensional metal *Phys. Rev.* B **57** R13997–9

[64] Laad M S, Bradaric I and Kusmartsev F V 2008 Orbital non-Fermi-liquid behavior in cubic ruthenates *Phys. Rev. Lett.* **100** 096402

[65] Ying Y A, Liu Y, He T and Cava R J 2011 Magnetotransport properties of $BaRuO_3$: observation of two scattering rates *Phys. Rev.* B **84** 233104

[66] Nair S, Wirth S, Friedemann S, Steglich F, Si Q and Schofield A J 2012 Hall effect in heavy fermion metals *Adv. Phys.* **61** 583–664

[67] Nakajima Y, Izawa K, Matsuda Y, Uji S, Terashima T, Shishido H, Settai R, Onuki Y and Kontani H 2004 Normal-state Hall angle and magnetoresistance in quasi-2D heavy fermion $CeCoIn_5$ near a quantum critical point *J. Phys. Soc. Japan.* **73** 5–8

[68] Kang W N, Kim H-J, Choi E-M, Kim H J, Kim K H P, Lee H S and Lee S-I 2002 Hall effect in *c*-axis-oriented MgB_2 thin films *Phys. Rev.* B **65** 134508

[69] Ahadi K and Stemmer S 2017 Novel metal–insulator transition at the $SmTiO_3/SrTiO_3$ interface *Phys. Rev. Lett.* **118** 236803

[70] Marshall P B, Kim H and Stemmer S 2017 Disorder versus two transport lifetimes in a strongly correlated electron liquid *Sci. Rep.* **7** 10312

[71] Narduzzo A, Albert G, French M M J, Mangkorntong N, Nohara M, Takagi H and Hussey N E 2008 Violation of the isotropic mean free path approximation for overdoped $La_{2-x}Sr_xCuO_4$ *Phys. Rev.* B **77** 220502

[72] Coleman P, Schofield A J and Tsvelik A M 1996 How should we interpret the two transport relaxation times in the cuprates? *J. Phys.: Condens. Matter* **8** 9985–10015

[73] Zheleznyak A T, Yakovenko V M, Drew H D and Mazin I I 1998 Phenomenological interpretations of the ac Hall effect in the normal state of $YBa_2Cu_3O_7$ *Phys. Rev.* B **57** 3089–98

[74] Ong N P 1991 Geometric interpretation of the weak-field Hall conductivity in two-dimensional metals with arbitrary Fermi surface *Phys. Rev.* B **43** 193–201

[75] Stojkovic B P and Pines D 1997 Theory of the longitudinal and Hall conductivities of the cuprate superconductors *Phys. Rev.* B **55** 8576–95

[76] Barman H, Laad M S and Hassan S R 2018 Realization of a 'two relaxation rates' in the Hubbard–Falicov–Kimball model *Phys. Rev.* B **97** 075133

[77] Blake M and Donos A 2015 Quantum critical transport and the Hall angle in holographic models *Phys. Rev. Lett.* **114** 021601

[78] Alexandrov A S, Bratkovsky A M and Mott N F 1994 Hall effect and resistivity of high-T_c oxides in the bipolaron model *Phys. Rev. Lett.* **72** 1734–7

[79] Allen S J, Jalan B, Lee S, Ouellette D G, Khalsa G, Jaroszynski J, Stemmer S and MacDonald A H 2013

Conduction-band edge and Shubnikov–de Haas effect in low-electron-density $SrTiO_3$ *Phys. Rev.* B **88** 045114
[80] Wang Z *et al* 2016 Tailoring the nature and strength of electron–phonon interactions in the $SrTiO_3$(0 0 1) 2D electron liquid *Nat. Mater.* **15** 835–9
[81] Raghavan S, Schumann T, Kim H, Zhang J Y, Cain T A and Stemmer S 2016 High-mobility $BaSnO_3$ grown by oxide molecular beam epitaxy *APL Mater.* **4** 016106
[82] Moriya T and Ueda K 2003 Antiferromagnetic spin fluctuation and superconductivity *Rep. Prog. Phys.* **66** 1299–341
[83] García-Muñoz J L, Rodríguez-Carvajal J, Lacorre P and Torrance J B 1992 Neutron-diffraction study of $RNiO_3$ (R = La,Pr,Nd,Sm): electronically induced structural changes across the metal–insulator transition *Phys. Rev.* B **46** 4414–25
[84] Medarde M, Dallera C, Grioni M, Delley B, Vernay F, Mesot J, Sikora M, Alonso J A and Martinez-Lope M J 2009 Charge disproportionation in $RNiO_3$ perovskites (R = rare earth) from high-resolution x-ray absorption spectroscopy *Phys. Rev.* B **80** 245105
[85] Woodward P M 1997 Octahedral tilting in perovskites.1. Geometrical considerations *Acta Crystallogr.* B **53** 32–43
[86] Park H, Millis A J and Marianetti C A 2012 Site-selective Mott transition in rare-earth-element nickelates *Phys. Rev. Lett.* **109** 156402
[87] Subedi A, Peil O E and Georges A 2015 Low-energy description of the metal–insulator transition in the rare-earth nickelates *Phys. Rev.* B **91** 075128
[88] Zhou J S, Goodenough J B and Dabrowski B 2005 Pressure-induced non-Fermi-liquid behavior of $PrNiO_3$ *Phys. Rev. Lett.* **94** 226602
[89] Liu J *et al* 2013 Heterointerface engineered electronic and magnetic phases of $NdNiO_3$ thin films *Nat. Commun.* **4** 2714
[90] Kobayashi H, Ikeda S, Yoda Y, Hirao N, Ohishi Y, Alonso J A, Martinez-Lope M J, Lengsdorf R, Khomskii D I and Abd-Elmeguid M M 2015 Pressure-induced unusual metallic state in $EuNiO_3$ *Phys. Rev.* B **91** 195148
[91] Jaramillo R, Ha S D, Silevitch D M and Ramanathan S 2014 Origins of bad-metal conductivity and the insulator–metal transition in the rare-earth nickelates *Nat. Phys.* **10** 304–7
[92] Zhang J Y, Kim H, Mikheev E, Hauser A J and Stemmer S 2016 Key role of lattice symmetry in the metal–insulator transition of $NdNiO_3$ films *Sci. Rep.* **6** 23652
[93] Vailionis A, Boschker H, Siemons W, Houwman E P, Blank D H A, Rijnders G and Koster G 2011 Misfit strain accommodation in epitaxial ABO_3 perovskites: lattice rotations and lattice modulations *Phys. Rev.* B **83** 064101
[94] Allen S J *et al* 2014 Gaps and pseudo-gaps at the Mott quantum critical point in the perovskite rare earth nickelates *APL Mater.* **3** 062503
[95] Pfleiderer C, Julian S R and Lonzarich G G 2001 Non-Fermi-liquid nature of the normal state of itinerant-electron ferromagnets *Nature* **414** 427–30
[96] Emery V J and Kivelson S A 1995 Superconductivity in bad metals *Phys. Rev. Lett.* **74** 3253–6
[97] Allen P B 1980 Theory of resistivity 'saturation' *Superconductivity in d- and f-Band Metals* ed H Suhl and M B Maple (New York: Academic) pp 291–304
[98] Calandra M and Gunnarsson O 2002 Electrical resistivity at large temperatures: saturation and lack thereof *Phys. Rev.* B **66** 205105
[99] Calandra M and Gunnarsson O 2003 Violation of Ioffe–Regel condition but saturation of resistivity of the high-T_c cuprates *Europhys. Lett.* **61** 88–94
[100] Millis A J, Hu J and Sarma S D 1999 Resistivity saturation revisited: results from a dynamical mean field theory *Phys. Rev. Lett.* **82** 2354–7
[101] Chakraborty B and Allen P B 1979 Boltzmann theory generalized to include band mixing: a possible theory for 'resistivity saturation' in metals *Phys. Rev. Lett.* **42** 736–8
[102] Gunnarsson O, Calandra M and Han J E 2003 Colloquium: Saturation of electrical resistivity *Rev. Mod. Phys.* **75** 1085–99
[103] Deng X Y, Mravlje J, Zitko R, Ferrero M, Kotliar G and Georges A 2013 How bad metals turn good: spectroscopic signatures of resilient quasiparticles *Phys. Rev. Lett.* **110** 086401
[104] Hussey N E, Takenaka K and Takagi H 2004 Universality of the Mott–Ioffe–Regel limit in metals *Phil. Mag.* **84** 2847–64
[105] Ioffe A F and Regel A R 1960 Non-crystalline, amorphous and liquid electronic semiconductors *Prog. Semicond.* **4** 237–91
[106] Mott N F 1972 Conduction in non-crystalline systems IX. The minimum metallic conductivity *Phil. Mag.* **26** 1015–26
[107] Licciardello D C and Thouless D J 1975 Constancy of minimum metallic conductivity in two dimensions *Phys. Rev. Lett.* **35** 1475
[108] Caviglia A D, Gariglio S, Reyren N, Jaccard D, Schneider T, Gabay M, Thiel S, Hammerl G, Mannhart J and Triscone J M 2008 Electric field control of the $LaAlO_3$/$SrTiO_3$ interface ground state *Nature* **456** 624–7
[109] King P D C, Wei H I, Nie Y F, Uchida M, Adamo C, Zhu S, He X, Bozovic I, Schlom D G and Shen K M 2014 Atomic-scale control of competing electronic phases in ultrathin $LaNiO_3$ *Nat. Nanotechnol.* **9** 443–7
[110] Scherwitzl R, Gariglio S, Gabay M, Zubko P, Gibert M and Triscone J M 2011 Metal–insulator transition in ultrathin $LaNiO_3$ films *Phys. Rev. Lett.* **106** 246403
[111] Yoshimatsu K, Okabe T, Kumigashira H, Okamoto S, Aizaki S, Fujimori A and Oshima M 2010 Dimensional-crossover-driven metal–insulator transition in $SrVO_3$ ultrathin films *Phys. Rev. Lett.* **104** 147601
[112] Son J, Moetakef P, LeBeau J M, Ouellette D, Balents L, Allen S J and Stemmer S 2010 Low-dimensional Mott material: transport in ultrathin epitaxial $LaNiO_3$ films *Appl. Phys. Lett.* **96** 062114
[113] Hwang J, Son J, Zhang J Y, Janotti A, Van de Walle C G and Stemmer S 2013 Structural origins of the properties of rare earth nickelate superlattices *Phys. Rev.* B **87** 060101
[114] Bergmann G 1984 Weak localization in thin films: a time-of-flight experiment with conduction electrons *Phys. Rep.* **107** 1–58
[115] Gurvitch M 1981 Ioffe–Regel criterion and resistivity of metals *Phys. Rev.* B **24** 7404–7
[116] Peil O E, Ferrero M and Georges A 2014 Orbital polarization in strained $LaNiO_3$: structural distortions and correlation effects *Phys. Rev.* B **90** 045128
[117] Wu M *et al* 2013 Strain and composition dependence of orbital polarization in nickel oxide superlattices *Phys. Rev.* B **88** 125124
[118] Lin X, Rischau C W, Buchauer L, Jaoui A, Fauque B and Behnia K 2017 Metallicity without quasi-particles in room-temperature strontium titanate *NPJ Quantum Mater.* **2** 41
[119] Wunderlich W, Ohta H and Koumoto K 2009 Enhanced effective mass in doped $SrTiO_3$ and related perovskites *Physica* B **404** 2202–12
[120] Eagles D M, Georgiev M and Petrova P C 1996 Explantation for the temperature dependence of plasma frequencies in $SrTiO_3$ using mixed-polaron theory *Phys. Rev.* B **54** 22–5

[121] van Mechelen J L M, van der Marel D, Grimaldi C, Kuzmenko A B, Armitage N P, Reyren N, Hagemann H and Mazin I I 2008 Electron–phonon interaction and charge carrier mass enhancement in $SrTiO_3$ *Phys. Rev. Lett.* **100** 226403

[122] Prange R E and Kadanoff L P 1964 Transport theory for electron–phonon interactions in metals *Phys. Rev.* **134** A566–80

[123] Devillers M A C 1984 Lifetime of electrons in metals at room temperature *Solid State Commun.* **49** 1019–22

[124] Du X, Tsai S-W, Maslov D L and Hebard A F 2005 Metal–insulator-like behavior in semimetallic bismuth and graphite *Phys. Rev. Lett.* **94** 166601

[125] Bruin J A N, Sakai H, Perry R S and Mackenzie A P 2013 Similarity of scattering rates in metals showing T-linear resistivity *Science* **339** 804–7

[126] Cain T A, Kajdos A P and Stemmer S 2013 La-doped $SrTiO_3$ films with large cryogenic thermoelectric power factors *Appl. Phys. Lett.* **102** 182101

Susanne Stemmer is Professor of Materials at the University of California, Santa Barbara. She did her doctoral work at the Max-Planck Institute for Metals Research in Stuttgart (Germany) and received her degree from the University of Stuttgart in 1995. Her research interests are in the development of scanning transmission electron microscopy techniques, molecular beam epitaxy, functional and strongly correlated oxide heterostructures, and topological materials. She has authored or co-authored more than 240 publications. Honors include election to Fellow of the American Ceramic Society, Fellow of the American Physical Society, Fellow of the Materials Research Society, Fellow of the Microscopy Society of America, and a Vannevar Bush Faculty Fellowship of the Department of Defense.